Fracture mechanics analysis of coating/substrate systems Part I: Analysis of tensile and bending experiments

Sung-Ryong Kim[a], **John A. Nairn**[b,*]
[a] *Sam Yang R&D Center, 63-2 Whaam-Dong, Yusung-gu, Taejon, South Korea*
[b] *Material Science and Engineering, University of Utah, Salt Lake City, Utah 84112, USA*

Received 30 December 1998; received in revised form 2 December 1999; accepted 7 Decemeber 1999

Abstract

A finite fracture mechanics model is used to predict the development of multiple cracks in the coating layer of coating/substrate systems. The stresses in a cracked coating are evaluated by a variational mechanics approach. These stresses are then used to calculate the total energy released due to the formation of a complete crack in the coating layer. The analysis can handle tensile loads or bending loads and includes the effect of residual thermal stresses. By assuming the next coating crack forms when the energy released due to the formation of a complete microcrack equals the *in situ* fracture toughness of coating, it is proposed that one can predict the number of coating cracks as a function of applied strain. Alternatively, it is proposed that experimental data for number of cracks *vs.* strain can be fit to the fracture analysis and be used to determine an *in situ* coating fracture toughness.

Keywords: Fracture Mechanics; Variational Mechanics; Coatings; Paints

1. Introduction

Coating or paint layers are often applied to the surfaces of polymeric, metallic, or composite structures. Coating layers are used for many reasons such as for protection, for decoration, for a barrier, or to provide unique surface properties. If the coating fails, it may cease to provide its' function and the system has therefore failed. Failure here is not in the sense of structural failure, but rather failure of the intended purpose of the coating. For example, a cracked paint layer ceases to provide an attractive surface appearance.

Coatings are not used for their loading bearing contributions. As a result, when a coated structure is subjected to loads, cracks typically develop within the coating before the substrate fails. Coating cracks usually initiate and rapidly propagate throughout the entire thickness of the coating. When the crack reaches the coating/substrate interface, it has several alternative failure modes [1–3]. The possibilities are surface embrittlement, where the crack enters the substrate causing substrate failure [4–8], coating delamination, where the crack turns and runs along the coating/substrate interface, and multiple cracking [1, 2, 3, 9], where the crack arrests but new cracks may form elsewhere after additional loading.

This study considers only multiple cracking of coatings in coating/substrate systems subjected to tension or to pure bending with the coating on the tension side of the specimen. During multiple cracking, individual coating cracks become arrested at the interface between the coating and substrate. Further loading of the sample causes additional cracks in the coating. The typical experiment is to count the number of coating cracks as a function of applied load [1–3]. The goal of fracture analysis of multiple cracking is to be able to predict such experiments and to be able to account for specimen effects such as substrate and coating thermomechanical properties and thickness.

Characterization of coatings are commonly done on free-films [10, 11]. For example, such studies may measure the strain-to-failure of the free film and then assume the coating on a substrate will fail when the

*Corresponding author. Tel.: +1-801-581-3413; fax: +1-801-581-4816
E-mail address: john.nairn@m.cc.utah.edu (J. A. Nairn).

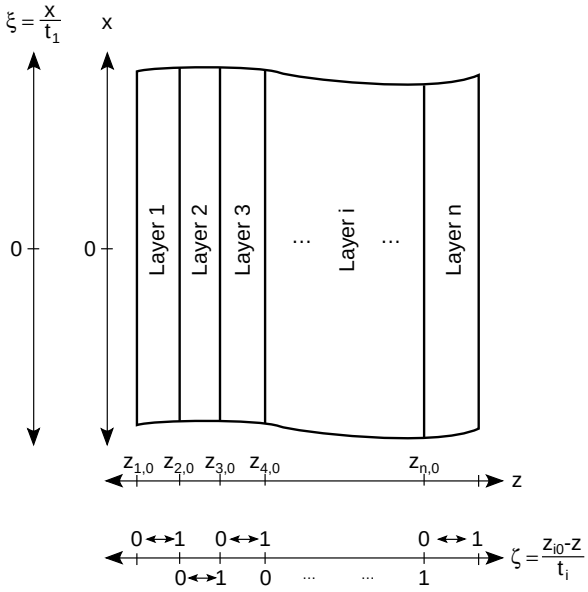

Fig. 1. The coordinate system of a multilayered system having n layers. The axial direction is the x axis and the thickness direction is the z axis. The ξ and ζ coordinates are dimensionless directions located along the x and z axes, respectively.

surface strain reaches the critical film strain. Such an approach does not work well. It has been observed that free-film failure and *in situ* failure can be drastically different. The free-film experiments do not account for substrate effects on the coating such as adhesion effects, residual stresses, and mechanical constraint on the deformation process of the coating. Even the use of an *in situ* coating failure strain cannot account for thickness affects [12]. It has commonly been observed that thick coatings can fail at significantly lower strain than thin coatings even when applied to identical substrates [12].

In this paper we derive a fracture analysis of coatings based on energy methods. In brief, we assume the next coating crack forms when the total energy released by the coating crack fracture event exceeds a critical value denoted as the *in situ* fracture toughness of the coating. The energy release rate is derived using variational mechanics and minimization of complementary energy. The final result is a closed-form, analytical solution for energy release rate due to formation of a complete coating crack. The analysis works for both tensile loading and pure bending and accounts for the possibility of residual stresses in all layers. A similar analysis for tensile loading only was presented in Ref. [1]. The analysis here corrects an error in that paper and extends the approach to more general specimens and to more general loading conditions such as bending. A prior analysis for bending loads is in Ref. [3]; the analysis here improves on that analysis and extends it to include residual thermal stresses. The original analyses [1, 3] and the analysis in this paper are all based on variational mechanics methods; McCartney has since solved a similar problem for both tensile and bending loads using approximate elasticity methods [14, 15]. Some sample problems are considered in the discussion section. The application of this fracture analysis to interpretation of experimental results is given in a separate publication [13].

2. Multilayered Structure Stress Analysis

2.1. Admissible Stress State

Consider an undamaged multilayered sample having n layers under an arbitrary initial stress state in the x-z plane. An edge view of the structure is illustrated in Fig. 1. The x direction is parallel to the axial direction of the layers and the z direction is transverse to the layers. The stress function for the initial stress state ($\Phi_0^{(i)}$) is defined using an initial stress function ($\phi^{(i)}$) in dimensionless units ξ and ζ defined by

$$\Phi_0^{(i)}(\xi,\zeta) = t_i^2\phi^{(i)}(\xi,\zeta) \tag{1}$$

where t_i is the thickness of layer i, the dimensionless ξ direction coordinate is $\xi = x/t_*$ where t_* is any conveniently chosen normalization length, and the dimensionless ζ direction coordinate is $\zeta = (z - z_0^{(i)})/t_i$ where $z_0^{(i)}$ is the z coordinate at the start of layer i. Using this initial stress function, the initial stress state is given by:

$$\sigma_{xx,0}^{(i)} = \phi_{\zeta\zeta}^{(i)}, \qquad \sigma_{xz,0}^{(i)} = -\lambda_i\phi_{\xi\zeta}^{(i)}, \qquad \textit{and} \qquad \sigma_{zz,0}^{(i)} = \lambda_i^2\phi_{\xi\xi}^{(i)} \tag{2}$$

where $\lambda_i = t_i/t_*$, the subscripts on $\phi^{(i)}$ indicate partial differentiation with respect to the dimensionless variables, and the "0" subscripts on the stresses imply initial stresses.

We next seek to find the stress state after the multilayered sample becomes damaged; specifically, we are considering damage in the form of cracks normal to the x axis each of which spans the full thickness of one or more layers. When such damage occurs, the initial stress state will change. We introduce one and only one assumption; we assume that the *change* in the x-axis tensile stress in each layer is proportional to the initial x-axis tensile stress where the proportionality function is a layer-dependent scaling function that depends only on ξ and is independent of ζ. Writing $-\psi_i(\xi)$ as the scaling function in layer i, the x axis tensile stresses after damage are assumed to be:

$$\sigma_{xx}^{(i)} = \phi_{\zeta\zeta}^{(i)}(1 - \psi_i(\xi)) \tag{3}$$

Here, we will only consider initial stress states that are independent of ξ. Two important initial stress states that are independent of ξ are initial uniform tension, where all initial stresses are constant, and pure bending about the x axis, where all initial stresses are linear in z. We further note that each component of stress can be written as

$$\sigma_{ij}^{(i)} = \sigma_{ij,0}^{(i)} + \sigma_{ij,p}^{(i)} \tag{4}$$

where $\sigma_{ij,0}^{(i)}$ are the initial stresses and $\sigma_{ij,p}^{(i)}$ are the perturbation stresses or the change in stresses caused by the introduction of transverse cracks in the layers. As shown in the Appendix using only the assumption in Eq. (3), the perturbation stress can be written as

$$\sigma_{xx,p}^{(i)} = -\Psi_i\omega_{i,\zeta\zeta} \tag{5}$$

$$\sigma_{xz,p}^{(i)} = \lambda_i\Psi_i'\omega_{i,\zeta} + \sum_{j=1}^{i-1}\lambda_j\Psi_j' \tag{6}$$

$$\sigma_{zz,p}^{(i)} = -\lambda_i^2\Psi_i''\omega_i - \sum_{j=1}^{i-1}\lambda_j\Psi_j''\left(\lambda_i\zeta + \lambda_{ji} + \lambda_j\left\langle\omega_{j,\zeta}\right\rangle\right) \tag{7}$$

where

$$\omega_i(\zeta) = \frac{\int_0^\zeta d\zeta'\int_0^{\zeta'} d\zeta''\phi_{\zeta\zeta}^{(i)}}{\left\langle\phi_{\zeta\zeta}^{(i)}\right\rangle}, \qquad \Psi_i(\xi) = \psi_i\left\langle\phi_{\zeta\zeta}^{(i)}\right\rangle, \qquad \text{and} \qquad \lambda_{ji} = \sum_{k=j+1}^{i-1}\lambda_k \tag{8}$$

and due to force and moment balance, the layer Ψ_i's and $\omega_i(\zeta)$'s are related by

$$\sum_{i=1}^{n}\lambda_i\Psi_i = 0 \tag{9}$$

$$\sum_{i=1}^{n-1}\lambda_i\Psi_i\left(\lambda_i\left\langle\omega_{i,\zeta}\right\rangle - \lambda_n\left\langle\omega_{n,\zeta}\right\rangle + \lambda_{in+1}\right) = 0 \tag{10}$$

Here averaging brackets denotes averaging over the thickness of layer i.

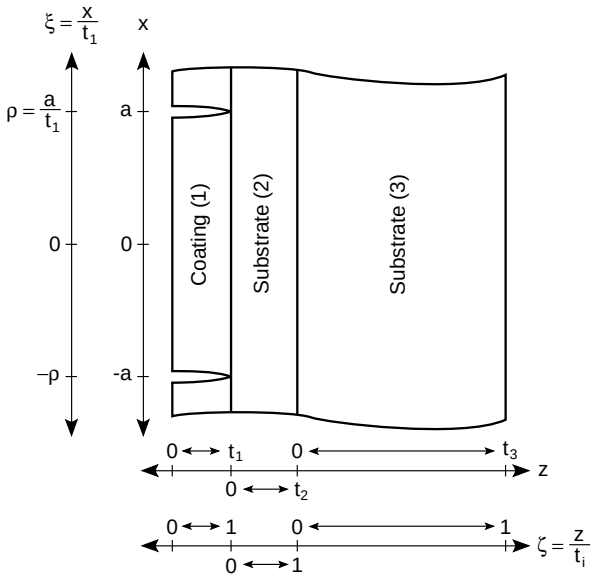

Fig. 2. The coordinate system between two cracks located at $x = \pm a$ in the coating (layer 1). The substrate is divided into two layers—layers 2 and 3. The axial direction is the x-axis and the thickness direction is the z-axis. The ξ and ζ coordinates are dimensionless directions located along the x and z axes, respectively.

2.2. Complementary Energy

In variational mechanics analysis of multilayered specimens, we can find the unknown layer functions, Ψ_i by minimizing the complementary energy. The Appendix gives a general result for the complementary energy for a n-layered specimen with x-independent initial stresses. Our interest is in analyzing a coating/substrate structure of a thin coating on a thick substrate. Now, the n layers for the analysis in the Appendix need not actually correspond to physical layers. We could, in principle, subdivide each physical layer into any number of layers. In the limit of a large number of layers, the variational solution would approach the exact solution. To get analytical results, however, we are only able to consider a small number of layers. As illustrated in Fig. 2, we modeled the coating/substrate system using three layers ($n = 3$). All layers are assumed to be isotropic, linear elastic solids; the extension to anisotropic layers is trivial. Layer 1 is the coating and it has modulus E_c, Poisson's ratio ν_c, and thickness t_1; layers 2 and 3 are in the substrate and they each have a modulus E_s, Poisson's ratio ν_s, and their thicknesses are t_2 and t_3.

Using force and moment balance (see Eqs. (9) and (10)), we can eliminate two of the three Ψ_i function in a three-layered specimen. Hence, $n = 3$ is the ideal choice for analysis of coating/substrate systems. Any fewer layers would have no unknown functions after satisfying force and moment balance; any more layers would lead to more than one Ψ_i function that would probably prohibit a closed-form solution. Applying the general n-layer result in the Appendix (see Eq. (85)) to a three-layered structure, eliminating Ψ_2 and Ψ_3 using Eqs. (9) and (10), and using $t_1 = t_*$ as the scaling dimension gives

$$\Gamma_p = W t_1^2 \left\langle \sigma_{xx,0}^{(1)} \right\rangle^2 \int_{\xi_i}^{\xi_f} d\xi \Big(C_1 \psi^2 + C_2 \psi'' \psi + C_3 \psi''^2 + C_4 \psi'^2 \Big) \tag{11}$$

where $\psi = \Psi_1 / \left\langle \sigma_{xx,0}^{(1)} \right\rangle$ is the dimensionless scaling function for the coating layer (ψ_1 with the subscript 1 now dropped),

$$C_i = \lambda_1 C_{i,111} + C'_{i,311} - \frac{\lambda_1 Q}{\lambda_2} C'_{i,312} - \frac{\lambda_1 Q}{\lambda_2} C'_{i,321} + \frac{\lambda_1^2 Q^2}{\lambda_2^2} C'_{i,322} \tag{12}$$

$$C'_{m,3jk} = \lambda_2 C_{m,2jk} + \lambda_3 C_{m,3jk} - \lambda_k C_{m,3j3} - \lambda_j C_{m,33k} + \frac{\lambda_j \lambda_k C_{m,333}}{\lambda_3} \tag{13}$$

$$Q = \frac{\lambda_1 \langle \omega_{1,\zeta} \rangle + \lambda_2 + \lambda_3 \big(1 - \langle \omega_{3,\zeta} \rangle\big)}{\lambda_2 \langle \omega_{2,\zeta} \rangle + \lambda_3 \big(1 - \langle \omega_{3,\zeta} \rangle\big)} \tag{14}$$

and $C_{m,ijk}$ is defined in the Appendix. The constants C_1 to C_4 evaluate explicitly to:

$$C_1 = \frac{1}{2}\left[K_{xx}^{(1)} \langle \omega_{1,\zeta\zeta}^2 \rangle + \frac{Q^2}{\lambda_2} K_{xx}^{(2)} \langle \omega_{2,\zeta\zeta}^2 \rangle + \frac{(1-Q)^2}{\lambda_3} K_{xx}^{(3)} \langle \omega_{3,\zeta\zeta}^2 \rangle\right] \tag{15}$$

$$\begin{aligned} C_2 = {} & K_{xz}^{(1)} \big(\langle \omega_{1,\zeta} \rangle - \langle \omega_{1,\zeta}^2 \rangle\big) - K_{xz}^{(2)} Q \Big(\lambda_2 \big(1 - (1+Q) \langle \omega_{2,\zeta} \rangle + Q \langle \omega_{2,\zeta}^2 \rangle\big) + \langle \omega_{1,\zeta} \rangle\Big) \\ & - K_{xz}^{(3)} (1-Q) \Big(\lambda_3 (1-Q) \big\langle (1-\omega_{3,\zeta})^2 \big\rangle + \lambda_2 \big(1 - Q \langle \omega_{2,\zeta} \rangle\big) + \langle \omega_{1,\zeta} \rangle\Big) \end{aligned} \tag{16}$$

$$\begin{aligned} C_3 = {} & \frac{K_{zz}^{(1)}}{2} \langle \omega_1^2 \rangle + \frac{\lambda_2 K_{zz}^{(2)}}{6} \left[\lambda_2^2 \left(1 - 6Q \langle \omega_2 \zeta \rangle + 3Q^2 \langle \omega_2^2 \rangle\right) + 3 \langle \omega_{1,\zeta} \rangle \left(\lambda_2 + \langle \omega_{1,\zeta} \rangle - 2Q\lambda_2 \langle \omega_2 \rangle\right)\right] \\ & + \frac{\lambda_3 K_{zz}^{(3)}}{2} \Bigg\{ \lambda_3^2 (1-Q)^2 \left(\frac{1}{3} - 2 \langle \omega_3 \zeta \rangle + \langle \omega_3^2 \rangle\right) \\ & + \big(\lambda_2 (1 - Q \langle \omega_{2,\zeta} \rangle) + \langle \omega_{1,\zeta} \rangle\big) \left[\lambda_2 (1 - Q \langle \omega_{2,\zeta} \rangle) + \langle \omega_{1,\zeta} \rangle + \lambda_3 (1-Q) - 2\lambda_3 \langle \omega_3 \rangle (1-Q)\right] \Bigg\} \end{aligned} \tag{17}$$

$$C_4 = \frac{1}{2}\left[K_{ss}^{(1)} \langle \omega_{1,\zeta}^2 \rangle + \lambda_2 K_{ss}^{(2)} \big\langle (1 - \omega_{2,\zeta} Q)^2 \big\rangle + \lambda_3 K_{ss}^{(3)} (1-Q)^2 \big\langle (1 - \omega_{3,\zeta})^2 \big\rangle\right] \tag{18}$$

3. Fracture Mechanics of Multiple Cracking in the Coating Layer

We applied the general results of the previous section to the problem of multiple cracking in a coating. Consider a coating/substrate specimen subjected to constant normal force resultant N and constant moment resultant M as illustrated in Fig. 3. For many coating systems with sufficiently good adhesion between the substrate and the coating, such loading will lead to multiple cracks in the coating. Because of the uniform loading conditions, the cracks will tend towards being periodic. It suffices to analyze the stresses within a unit-cell of damage or the zone between two coating cracks as illustrated in Fig. 2. The two cracks in the coating are located at $\pm a$ or in dimensionless units at $\pm\rho$ where $\rho = a/t_1$. By the calculus of variations, the Euler equation for minimizing the complementary energy in Eq. (11) is

$$\frac{\partial^4 \psi}{\partial \xi^4} + p \frac{\partial^2 \psi}{\partial \xi^2} + q\psi = 0 \tag{19}$$

where

$$p = \frac{C_2 - C_4}{C_3} \qquad \text{and} \qquad q = \frac{C_1}{C_3} \tag{20}$$

This differential equation has already been solved for analysis of other multiple cracking problems [16–22]. Two examples are matrix cracking in the central plies of cross-ply laminates [16–21] and fiber breaks in single-fiber fragmentation experiments [22]. The solutions for all possible values or p and q are given in the Appendix.

For fracture mechanics calculations we need to calculate the total strain energy which is equivalent to the complementary energy when there are traction-only loading conditions. Thus strain energy can be evaluated by substituting the solution for ψ into Eq. (11) and integrating. Hashin has shown, however, that the integration process is greatly simplified by multiplying Eq. (19) by ψ and integrating, by parts, from $-\rho$ to ρ [16]. Using this approach, the strain energy for a single crack interval is quickly derived to be

$$U = U_0 + 2C_3 t_1^2 W \left\langle \sigma_{xx,0}^{(1)} \right\rangle^2 \chi(\rho) \tag{21}$$

where U_0 is the strain energy in the absence of damage and $\chi(\rho) = -\psi'''(\rho)$. The function $\chi(\rho)$ is given in the Appendix.

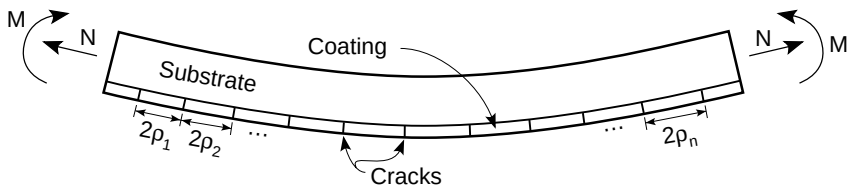

Fig. 3. A coating/substrate system subjected to normal force N and constant bending moment M. The coating is on the tension side of the beam and has cracked into multiple crack intervals characterized by dimensionless spacings ρ_1, ρ_2, $\cdots$, ρ_n.

We next consider a sample of length L having n crack intervals in the coating characterized by dimensionless spacings ρ_1, ρ_2, ..., ρ_n (see Fig. 3). Summing the energy for all crack intervals, the total strain energy can be written as

$$U = U_0 + C_3 t_1 \left\langle \sigma^{(1)}_{xx,0} \right\rangle^2 LW \frac{\sum_{i=1}^{n} \chi(\rho_i)}{\sum_{i=1}^{n} \rho_i} \tag{22}$$

where U_0 is now the total strain energy in the absence of damage and the specimen length can be written as $L = \sum_{i=1}^{n} 2\rho_i t_1$.

3.1. Mechanical Energy Release Rate

Coating/substrate systems are typically made from materials with different thermal expansion coefficients. Thus, commonly there will be residual stresses that influence the failure of the coating. We initially, however, ignore residual stresses and calculate the energy release rate for cracking in the coating due only to mechanically applied loads. The effect of residual stresses is calculated next section. The energy release rate for crack growth is

$$G = \frac{\partial \Omega}{\partial A} - \frac{\partial U}{\partial A} \tag{23}$$

where Ω is external work and A is crack area. For traction-only loading and in the absence of residual stresses, it can be shown that

$$\frac{\partial \Omega}{\partial A} = 2\frac{\partial U}{\partial A} \qquad \text{or} \qquad G = \frac{\partial U}{\partial A} \tag{24}$$

Differentiating Eq. (22), the mechanical-only energy release rate is

$$G_{mech} = C_3 t_1 \left\langle \sigma^{(1)}_{xx,m0} \right\rangle^2 Y(D) \tag{25}$$

where

$$Y(D) = LW \frac{d}{dA} \frac{\sum_{i=1}^{n} \chi(\rho_i)}{\sum_{i=1}^{n} \rho_i} \tag{26}$$

and $D = n/L$ is the crack density in the coating. Note that Eq. (25) was derived assuming mechanical stresses only; the subscript m in $\left\langle \sigma^{(1)}_{xx,m0} \right\rangle$ indicates the initial mechanical stresses.

3.2. Total Energy Release Rate

The total energy release rate is the energy release rate due to both mechanical and residual stresses. The coating cracks typically form normal to the applied loads and thus are mode I cracks. It has recently been

proven that the total energy release rate for mode I cracking in composites can be derived exactly from a purely mechanical stress analysis [23]. In other words, the effect of residual stresses can be included without any need for conducting a thermoelasticity analysis. From Ref. [23] the total energy release rate including residual stresses is

$$G_I = G_{mech}\left(1 + \frac{\Delta T}{2}\frac{\sum_{i=1}^{r} V_i \boldsymbol{\alpha}^{(i)} \cdot \frac{d\overline{\boldsymbol{\sigma}^{(im)}}}{dA}}{G_{mech}}\right)^2 \tag{27}$$

where $\Delta T = T_s - T_0$ is the difference between the specimen temperature and the stress-free temperature, the sum is over r phases in the composite, V_i is the volume of phase i, $\boldsymbol{\alpha}^{(i)}$ is the thermal expansion tensor of phase i, and $\overline{\boldsymbol{\sigma}^{(im)}}$ is the phase-averaged *mechanical* stress in phase i:

$$\overline{\boldsymbol{\sigma}^{(im)}} = \frac{1}{V_i}\int_{V_i} \boldsymbol{\sigma}^m dV \tag{28}$$

In applying Eq. (27) to the coating/substrate system, we treat the structure as a two-phase composite. In this plane-stress, bending analysis, the phase-average transverse stresses are identically zero and the axial stresses must obey force balance or

$$0 = \overline{\sigma_{zz}^{(1m)}} = \overline{\sigma_{zz}^{(2m)}} = \overline{\sigma_{yy}^{(1m)}} = \overline{\sigma_{yy}^{(2m)}} \tag{29}$$

$$V\sigma_0 = V_1\overline{\sigma_{xx}^{(1m)}} + V_2\overline{\sigma_{xx}^{(2m)}} \tag{30}$$

where V is total volume of the specimen and σ_0 is the applied axial load in the x direction. Substituting into Eq. (27) and using the geometry of the coating/substrate system

$$G_{total} = G_{mech}\left(1 + \frac{\Delta\alpha\Delta T}{2}\frac{\frac{d}{dA}\int_{V_1}\overline{\sigma_{xx}^{(1m)}}dV}{G_{mech}}\right)^2 \tag{31}$$

The phase average mechanical stress in the coating evaluates to

$$\int_{V_1}\overline{\sigma_{xx}^{(1m)}}dV = Wt_1^2\left\langle\sigma_{xx,m0}^{(1)}\right\rangle\sum_{i=1}^{n}\int_{-\rho_i}^{\rho_i}(1-\psi)d\xi = 2Wt_1^2\left\langle\sigma_{xx,m0}^{(1)}\right\rangle\sum_{i=1}^{n}\left(\rho_i - \frac{C_3\chi(\rho_i)}{C_1}\right) \tag{32}$$

The integration required for Eq. (32) can be derived by direct integration of ψ or by integration of the Euler Equation in Eq. (19) from $-\rho_i$ to ρ_i. Finally, substitution of G_{mech} in Eq. (25) and Eq. (32) into Eq. (31) gives

$$G_{total} = C_3 t_1\left(\left\langle\sigma_{xx,m0}^{(1)}\right\rangle - \frac{\Delta\alpha\Delta T}{2C_1}\right)^2 Y(D) \tag{33}$$

Physically, the term $-\Delta\alpha\Delta T/2C_1$ is the initial residual stress in the coating layer before any damage. Thus the squared term in Eq. (33) is the sum of the initial mechanical and initial residual stresses in the coating or the total initial stress in the coating.

3.3. Finite Fracture Mechanics Analysis

To evaluate energy release rate for cracking in coatings we need to evaluate $Y(D)$. $Y(D)$ can be converted to a crack density derivative by using the relation $A = nt_1W = LWt_1D$. Substitution into Eq. (26) gives

$$Y(D) = 2\frac{d}{dD}\Big(D\left\langle\chi(\rho)\right\rangle\Big) \tag{34}$$

where

$$\left\langle\chi(\rho)\right\rangle = \frac{1}{n}\sum_{i=1}^{n}\chi(\rho_i) \tag{35}$$

is the average value of $\chi(\rho)$. Equation (34) differs by a factor of two from the comparable equation in Ref. [1] (see Eq. (36) in Ref. [1]). This new result corrects an error in Ref. [1] in the conversion from crack area (A) to crack density (D).

Now, $Y(D)$ could be further evaluated by analytical differentiation of $\chi(\rho)$. This approach, however, was shown to give very poor results when predicting microcracking in laminates [19, 20]. Physically, the analytical differentiation is treating the crack density as a continuous variable. Multiple cracking in coatings, however, occurs as a series of fracture events where the events are formations of complete cracks. We thus instead calculate the energy release rate for the formation of a complete crack. This result is found by evaluating $Y(D)$ as a *discrete* derivative. If the next cracks forms in the middle of a crack interval characterized by crack spacing ρ_k, $Y(D)$ evaluates to

$$Y(D) = 2\frac{\Delta\Big(D\,\langle\chi(\rho)\rangle\Big)}{\Delta D} = 2\big(2\chi(\rho_k/2) - \chi(\rho_k)\big) \tag{36}$$

Because coating cracks tend to be periodic, we could further replace ρ_k by the average value of $\rho = 1/(2t_1D)$ to get a simple result for $Y(D)$ that depends only on the current crack density.

To predict multiple cracking in coatings we assume that the next crack forms when the energy release rate for formation of the next crack is equal to the critical energy release rate, G_c, or toughness of the coating. The crack density as a function of applied stress can then be related to crack density by equating G_{total} in Eq. (33) to G_c and solving for $\left\langle \sigma^{(1)}_{xx,m0} \right\rangle$. This approach differs from conventional fracture mechanics because it deals with a fracture event instead of an infinitesimal amount of crack growth. A similar approach, however, was shown to work well for analysis of microcracking in composite laminates [20]. The approach of using energy release rate for fracture events to predict failure has been used implicitly by numerous authors. Hashin has recently discussed the topic and suggested naming the method *Finite Fracture Mechanics* [24]. The rationale is that some materials, particularly composite materials, fail by a series of events rather than by slow crack growth. Because it is impossible to follow crack growth, there is little incentive to develop traditional fracture mechanics analyses for those unobservable phenomena. Instead, Finite Fracture Mechanics is proposed as a potential approach for using energy methods to analyze observed failures. There are experimental results suggesting that Finite Fracture Mechanics works well for some failure processes [19, 20, 24].

3.4. Final Evaluation of Required Constants

By using Finite Fracture Mechanics and G_{total} in Eq. (33), one can predict multiple cracking as a function of applied stress. In other words, Eq. (33) completes the fracture mechanics analysis for multiple cracking in coatings. To actually use Eq. (33), however, we need to know C_1, C_2, C_3, and C_4 in terms of the mechanical and geometric properties of the coating/substrate system and in terms of the applied axial stress or bending moment. The explicit results for C_1, C_2, C_3, and C_4 are given in Eqs. (15)–(18); these results, however, depend on the functions ω_i which, in turn, depend on the initial stresses in the layers (see Eq. (8)). In this section we give the necessary results for finding all constants for simple tension or pure bending.

We consider tensile experiments first. Because a coating/substrate specimen is unsymmetric, axial loading by uniform stress will lead to some bending of the structure and bending stresses in the layers. Typical experiments, however, will be for specimens clamped and loaded in tension. Such loading will prevent the bending; instead there will be a net moment in the grips that compensates the bending. Thus, the result of tensile testing will be initial stresses that are constant within each layer, or the initial stresses are independent of both x and z. For such initial stresses we have

$$\omega_i = \frac{1}{2}\zeta^2, \qquad \omega_{i,\zeta} = \zeta, \qquad \text{and} \qquad \omega_{i,\zeta\zeta} = 1 \tag{37}$$

The required constants reduce to

$$C_1 = \frac{1}{2}\left[K^{(1)}_{xx} + \frac{Q^2}{\lambda_2}K^{(2)}_{xx} + \frac{(1-Q)^2}{\lambda_3}K^{(3)}_{xx}\right] \tag{38}$$

$$C_2' = \frac{1}{6}\left[K^{(1)}_{xz} - K^{(2)}_{xz}Q\big(3+\lambda_2(3-Q)\big) + K^{(3)}_{xz}\lambda_3(1-Q)^2\right] \tag{39}$$

$$C_3' = \frac{1}{120}\left\{3K_{zz}^{(1)} + K_{zz}^{(2)}\left[\lambda_2^3\left(20-15Q+3Q^2\right)+\lambda_2^2(30-10Q)+15\lambda_2\right]+3\lambda_3^3(1-Q)^2K_{zz}^{(3)}\right\} \quad (40)$$

$$C_4' = \frac{1}{6}\left[K_{ss}^{(1)} + \lambda_2 K_{ss}^{(2)}\left(Q^2-3Q+3\right)+\lambda_3 K_{ss}^{(3)}(1-Q)^2\right] \quad (41)$$

where Q reduces to

$$Q = 1 + \frac{\lambda_1+\lambda_2}{\lambda_2+\lambda_3} \quad (42)$$

These results are identical to the tensile loading results in Ref. [1] (note: the constants in Ref. [1] where given in terms or $R = Q - 1$ instead of in terms of Q).

In this plane stress analysis, the average mechanical stress in the coating during tensile loading is simply

$$\left\langle \sigma_{xx,m0}^{(1)} \right\rangle = \frac{E_c}{E_{0t}}\sigma_0 \quad (43)$$

where $E_{0t} = (E_c t_1 + E_s(t_2+t_3))/(t_1+t_2+t_3)$ is the rule-of-mixtures tensile modulus of the specimen in the x direction and σ_0 to the total applied axial stress. This result together with Eq. (33) gives an identical energy release rate to Ref. [1] except for the factor of 2 error in $Y(D)$ in Ref. [1] discussed above.

We finally consider pure bending with loading by net moment M. If we take the origin of the z axis to be the center of the beam, the coating to be on the negative z side of the beam, and define positive moment to be a moment leading to tension in the coating, a simple bending analysis of the two-layer, coating/substrate beam [25] gives the initial stresses in layer i as

$$\sigma_{xx}^{(i)} = -\frac{ME^{(i)}(z-z_N)}{E_cI_c + E_sI_s} \quad (44)$$

where $E^{(i)}$ is the modulus of layer i, z_N is the location of the neutral axis of the beam, and I_c and I_s are the bending moments of inertia for the coating and substrate layers about the neutral axis. By the parallel axis theorem, I_c and I_s are:

$$I_c = \frac{Wt_1^3}{12} + Wt_1\left(\frac{t_2+t_3}{2}+z_N\right)^2 \qquad \text{and} \qquad I_s = \frac{W(t_2+t_3)^3}{12} + W(t_2+t_3)\left(\frac{t_1}{2}-z_N\right)^2 \quad (45)$$

The location of the neutral axis is given by [25]:

$$z_N = \frac{t_1(\lambda_2+\lambda_3)}{2}\frac{(E_s-E_c)}{E_c+E_s(\lambda_2+\lambda_3)} \quad (46)$$

Converting to dimensionless units, we find the average stress function ($\omega_{i,\zeta\zeta}$) and its integrals to be

$$\omega_{i,\zeta\zeta} = \frac{2(\zeta-\zeta_N^{(i)})}{1-2\zeta_N^{(i)}}, \qquad \omega_{i,\zeta} = \frac{\zeta^2-2\zeta\zeta_N^{(i)}}{1-2\zeta_N^{(i)}}, \qquad \text{and} \qquad \omega_i = \frac{\zeta^3-3\zeta^2\zeta_N^{(i)}}{3(1-2\zeta_N^{(i)})} \quad (47)$$

where

$$\zeta_N^{(i)} = \frac{z_N - z_0^{(i)}}{t_i} \quad (48)$$

is the dimensionless coordinate of the neutral axis in layer i. Doing all the required integrations (with verification using Mathematica [26]) gives

$$\left\langle \omega_{i,\zeta\zeta}^2 \right\rangle = \frac{4(1-3\zeta_N^{(i)}+3{\zeta_N^{(i)}}^2)}{3(1-2\zeta_N^{(i)})^2} \quad (49)$$

$$\left\langle \omega_{i,\zeta} \right\rangle = \frac{1-3\zeta_N^{(i)}}{3(1-2\zeta_N^{(i)})} \quad (50)$$

$$\left\langle \omega_{i,\zeta}^2 \right\rangle = \frac{3-15\zeta_N^{(i)}+20{\zeta_N^{(i)}}^2}{15(1-2\zeta_N^{(i)})^2} \quad (51)$$

$$\left\langle (1-\omega_{i,\zeta})^2 \right\rangle = 1 - 2\left\langle \omega_{i,\zeta} \right\rangle + \left\langle \omega_{i,\zeta}^2 \right\rangle \tag{52}$$

$$\left\langle \omega_i^2 \right\rangle = \frac{5 - 35\zeta_N^{(i)} + 63{\zeta_N^{(i)}}^2}{315(1-2\zeta_N^{(i)})^2} \tag{53}$$

$$\left\langle \omega_i \right\rangle = \frac{1 - 4\zeta_N^{(i)}}{12(1-2\zeta_N^{(i)})} \tag{54}$$

$$\left\langle \omega_i \zeta \right\rangle = \frac{4 - 15\zeta_N^{(i)}}{60(1-2\zeta_N^{(i)})} \tag{55}$$

where the dimensionless coordinates for the neutral axis in each layer are

$$\zeta_N^{(1)} = \frac{h_N}{t_1}, \qquad \zeta_N^{(2)} = \frac{h_N - t_1}{t_2}, \qquad \text{and} \qquad \zeta_N^{(3)} = \frac{h_N - t_2 - t_1}{t_3} \tag{56}$$

where h_N is the height of the neutral axis above the free surface of the coating:

$$h_N = \frac{t_1}{2}\left[\frac{E_c + E_s(\lambda_2+\lambda_3)(2+\lambda_2+\lambda_3)}{E_c + E_s(\lambda_2+\lambda_3)}\right] \tag{57}$$

These results can be substituted into Eq. (14) and Eqs. (15)–(18) to determine Q and C_1 to C_4 for coating/substrate specimens loaded in pure bending.

Finally, the average, initial mechanical stress in the coating during bending loading is found by integrating Eq. (44) over the coating layer. The result is

$$\left\langle \sigma_{xx,m0}^{(1)} \right\rangle = -\frac{E_c}{E_{0b}}\frac{M\bar{z_1}}{I} \tag{58}$$

where

$$E_{0b} = \frac{E_c I_c + E_s I_s}{I} \tag{59}$$

is the effective bending modulus of the composite beam, $I = WB^3/12$ is the bending moment inertia of the full beam of thickness $B = t_1 + t_2 + t_3$, and

$$\bar{z_1} = -\left(\frac{t_2+t_3}{2}\right) - z_N \tag{60}$$

is the position of the midpoint of the coating relative to the neutral axis. Equation (58) together with Q and C_1 to C_4 for pure bending can be substituted into Eq. (33) to get the total energy release rate for formation of a complete crack in the coating layer.

4. Discussion and Conclusions

For some sample calculations, we consider a polymeric coating on a either a polymeric substrate or a steel substrate subjected to either tension loads or bending loads. The results for tension or bending are best compared by plotting the results as a function of strain. For tensile loading, the strain in the film is equal to the total applied strain or

$$\varepsilon_t = \frac{\sigma_0}{E_{0t}} \tag{61}$$

which gives

$$\left\langle \sigma_{xx,m0}^{(1)} \right\rangle = E_c \varepsilon_t \tag{62}$$

For bending loads, the applied moment, M, can be converted to an effective bending strain by calculating the maximum outer-surface strain in the equivalent homogeneous beam with bending modulus E_{0b}. The outer-surface strain on the tensile surface at $-B/2$ of the equivalent homogeneous beam is

$$\varepsilon_b = \frac{MB}{2E_{0b}I} \tag{63}$$

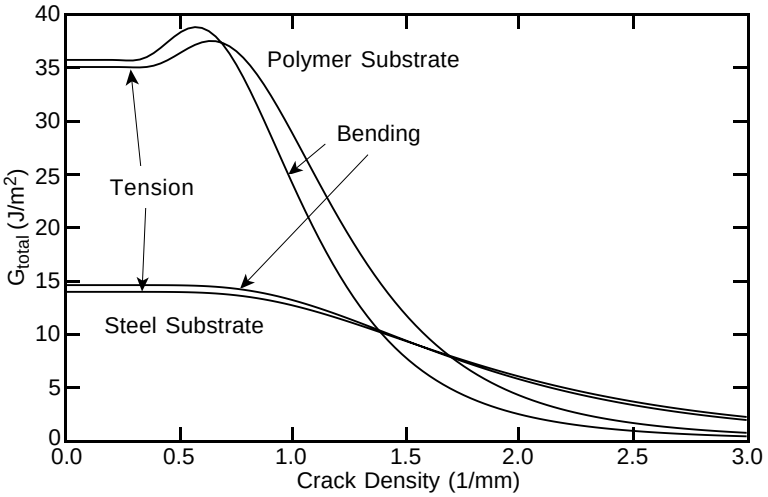

Fig. 4. G_{total} as a function of crack density for a polymeric coating on either a polymeric substrate or a steel substrate. For each substrate type, the specimens are loaded in tension or bending. The assumed specimen properties were $E_c = 1660$ MPa, $\nu_c = 0.33$, $t_c = 5$ mils, $E_s = 2500$ MPa (polymeric substrate), $E_s = 115000$ MPa (steel substrate), $\nu_s = 0.33$, and $t_s = 125$ mils. The applied strains were $\varepsilon_t = \varepsilon_b = 1\%$.

Substitution into Eq. (58) gives

$$\left\langle \sigma^{(1)}_{xx,m0} \right\rangle = -\frac{2\bar{z}_1}{B} E_c \varepsilon_b \tag{64}$$

For thin coatings, $\bar{z}_1 \approx -B/2$ and $\left\langle \sigma^{(1)}_{xx,m0} \right\rangle \approx E_c \varepsilon_b$ or the coating stress is approximately given by a layer subjected to the maximum surface bending strain. For thicker coatings, Eq. (64) corrects the average coating stress for variation in stress across the thickness of the coating.

We first calculated energy release rate G_{total} in Eq. (33) as a function of crack density. Although the analysis can handle anisotropic layers and residual stresses, for this sample calculation we assumed an isotropic coating layer with $E_c = 1660$ MPa and $\nu_c = 0.33$ on either an isotropic polymer substrate with $E_s = 2500$ MPa and $\nu_s = 0.33$ or an isotropic steel substrate with $E_s = 115000$ MPa and $\nu_s = 0.33$. Residual stresses were ignored for simplicity but can easily be included by evaluating $\Delta\alpha\Delta T/(2C_1)$ for the coating/substrate system. The substrate layer was subdivided such that $t_2 = t_1$ or that the layer next to the coating had the same thickness as the coating. t_2 could alternatively be selected by minimizing total complementary energy with respect to t_2, but this approach requires numerical calculations. Based on a few such numerical calculations, it was observed that the final result is not very sensitive to t_2 and that there is typically a broad minimum located near $t_2 = t_1$. The results for G_{total} as a function of crack density for a 0.127 mm (5 mil) coating on a 3.175 mm (125 mil) substrate at applied tensile or bending strain of $\varepsilon_t = \varepsilon_b = 1\%$ are given in Fig. 4. All curves have a characteristic shape of a constant high value of G_{total} at low crack density followed by a decrease in G_{total} at high crack density. The initial constant value at low crack density corresponds to the G_{total} for the initiation of cracking or the formation of the first crack. The value of G_{total} remains constant as long as the cracks are far apart and therefore do not interact. As the cracks get closer, they eventually influence each other and G_{total} drops.

There is a significant substrate effect. All other factors being equal, G_{total} is much higher at low crack density for the lower-modulus polymeric substrate than it is for the higher-modulus steel substrate. The situation reverses at high crack density. Thus for a coating with a given toughness, it might be expected to crack sooner on the polymeric substrate than on the steel substrate but to eventually develop more cracks on the steel substrate. The results for real coatings might be different, however, because the effective or *in situ* coating toughness might, itself, depend on the substrate. For example, if a steel substrate embrittles the coating layer, the cracks may form sooner when the coating is on the steel substrate than when it is on the polymeric substrate even though the G_{total} is lower. Some experiments aimed at measuring *in situ* coating toughness for paints on polymeric and steel substrates are described in a separate publication [13].

The G_{total} results are nearly the same for tensile or bending loading on a given substrate type. The

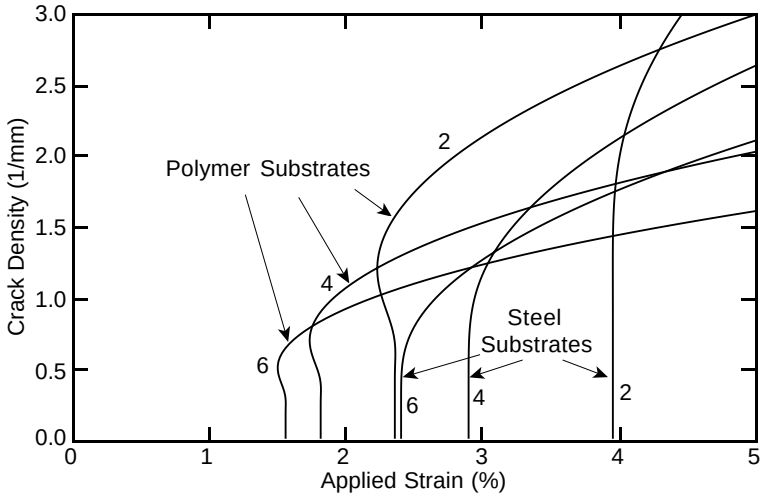

Fig. 5. Predicted crack density as a function of applied strain during bending tests for polymeric coatings (E_c = 1660 MPa and $\nu_c = 0.33$) of thicknesses 2, 4, or 6 mils on a polymeric substrate ($E_s = 2500$ MPa and $\nu_s = 0.33$) or a steel substrate ($E_s = 115000$ MPa and $\nu_s = 0.33$). All substrates were 125 mils thick. The coating toughness was assumed to be $G_c = 100$ J/m^2.

theoretical analyses for tensile or bending loads are significantly different, but when completed and plotted *vs.* effective strain in the coating layer, it is seen that energy release rate is controlled by the effective strain in the coating rather than the global loading method. The differences between tension and bending get more significant as the coating layer gets thicker. The results in Fig. 4 were for thin coatings. From an analysis point of view, coating experiments can be conducted either in tension or bending. Experimentally, however, the bending configuration has several advantages. First, the bending configuration focuses the highest stresses on the coating and promotes coating cracking before substrate failure or yielding. Second, bending experiments are usually easier. They use simpler fixturing and with proper choice of specimen dimensions, a desired bending strain ε_b can be achieved with a much lower absolute load than required to get the same tensile strain ε_t in tension.

Experimental observations will typically record coating crack density as a function of applied strain. If we assume the next coating crack forms when G_{total} becomes equal to the effective or *in situ* coating toughness, G_c, the experimental results can be predicted by solving Eq. (33) for applied strain. For tensile loading, the result is

$$\varepsilon_t = \frac{1}{E_c}\sqrt{\frac{G_c}{C_3 t_1 Y(D)}} + \frac{\Delta\alpha\Delta T}{2E_c C_1} \tag{65}$$

For bending loads, the result is

$$\varepsilon_b = -\frac{B}{2\bar{z}_1 E_c}\sqrt{\frac{G_c}{C_3 t_1 Y(D)}} - \frac{B\Delta\alpha\Delta T}{2\bar{z}_1 E_c C_1} \tag{66}$$

Figure 5 gives some sample calculations for crack density as a function of loading during bending tests of coatings on either polymeric or steel substrates. The coating and substrate properties are identical to the results described above. For each substrate, the predictions are given for coatings with thicknesses of 0.0508 mm (2 mils), 0.102 mm (4 mils) and 0.152 mm (6 mils). The coating toughness was assumed to be $G_c = 100$ J/m^2 on both substrates. For a given substrate there is a significant thickness effect. Thicker coatings are predicted to crack sooner while thinner coatings may eventually develop more cracks. The propensity of paints to crack sooner when they are thicker has long be recognized in the coatings industry [12]. The energy based analysis presented here is consistent with this experimental observation. Strength-based models which assume a coating fails when it reaches its strain-to-failure cannot not predict this important thickness effect.

As expected from the G_{total} calculations, the cracks form sooner with a polymeric substrate than with a steel substrate. Again, this prediction assumes that G_c is independent of the substrate. If, in fact, G_c depends on substrate and is lower when using steel substrates than when using polymeric substrates, it is possible for cracks to form sooner on steel substrates. The crack density predictions for polymeric substrates all have a small, non-physical region of negative slope in the rapidly rising portion of the curves which shows the strain decreasing as the crack density increases. This region is a consequence of plotting Eq. (66), which gives strain as a function of crack density, in a reverse plot that has crack density as a function of strain. In analysis of experiments, this negative slope region should be ignored. Instead, these curves predict that once cracks forms, the crack density will rapidly increase. The initial vertical rise of the predictions can be extended up until it intersects the curve again at which point the prediction is that higher strains will be required to get more cracks.

The predictions in Fig. 5 ignore residual stresses. The residual stresses can easily be included by evaluating $\Delta\alpha\Delta T/(2C_1)$ for any given coating/substrate system. The net result from Eqs. (65) and (66) will simply be a horizontal shift of each curve along the strain axis. The magnitude of the shift will depend on the coating thickness. If the residual stress term exceeds the strain to form the first microcrack, the curve may shift past the origin. Such a shift corresponds to the case where residual stresses alone induce coating cracking.

We close with some comments about applying this fracture analysis to experiments on real coatings. The fracture mechanics analysis assumes linear elastic materials and assumes that only the coating cracks. It further assumes perfect adhesion between the coating and the substrate. When these assumptions approximate real experiments, it should be possible to measure crack density as a function of applied strain and to fit to Eq. (65) or Eq. (66) to determine an *in situ* toughness for the coating. All calculations predict that soon after the first coating crack there should be a rapid increase in crack density until the cracks begin to interact with each other. Our experience with real coatings, however, is that the crack density increases slower than predicted [13]. Such a discrepancy may be a consequence of either statistical variations in initial flaws in the coating or to imperfect coating/substrate adhesion. For example if each coating crack induces a local delamination, that additional damage will increase the effective crack density (decrease the effective crack spacing) and therefore decrease the rate of subsequent cracking. A series of coating fracture experiments on polymeric and steel substrates are given in a separate publication [13].

The calculation of energy release rate from experimental data for crack density *vs.* strain requires a theoretical result for G_{total}. In principle, energy release rate can be measured entirely by experiment by determining the effect of coating cracks on specimen compliance. For most coating geometries, however, the change in compliance is too small to be resolved experimentally. One must therefore rely of theoretical results for G_{total}. A final concern is whether G_{total} in Eq. (33) is sufficiently accurate. We suggest that Eq. (33) is the most accurate result possible in a closed-form, analytical solution. Some techniques used when analyzing microcracking in laminates such as allowing the scaling function $\psi_i(\xi)$ to depend on ζ as well as ξ [27, 28] or subdividing each layer into multiple layers [29] may be useful for improving accuracy. These methods, however, require numerical calculations. Our experience with coating experiments suggests that further theoretical work would be more fruitfully directed towards including real material effects such as non-linear stress-strain properties or imperfect adhesion between the coating and the substrate rather than at improving the accuracy of the linear elastic, perfect adhesion solution.

Acknowledgment

This work was supported by a grant from the Mechanics of Materials program at the National Science Foundation (CMS-9713356). Some additional support was provided by the duPont company under the direction of Dr. Paul McGonigal.

5. Appendix

5.1. Perturbation Stresses

A general stress function that encompasses all possible stress states satisfying the assumption in Eq. (3) is given by:

$$\Phi^{(i)}(\xi,\zeta) = t_i^2\left(\phi^{(i)}(\xi,\zeta)(1-\psi_i(\xi)) + \psi_{i,a}(\xi)\zeta + \psi_{i,b}(\xi)\right) \tag{67}$$

where $\psi_{i,a}$ and $\psi_{i,b}$ are two arbitrary functions of only ξ. The x-axis tensile stress for this stress function is given by Eq. (3). The shear stress and z-axis tensile stress derived from the stress function in Eq. (67) are:

$$\sigma_{xz}^{(i)} = -\lambda_i\left(\phi_{\xi\zeta}^{(i)} - \frac{\partial}{\partial\xi}(\psi_i\phi_\zeta^{(i)} - \psi_{i,a})\right) \tag{68}$$

$$\sigma_{zz}^{(i)} = \lambda_i^2\left(\phi_{\xi\xi}^{(i)} - \frac{\partial^2}{\partial\xi^2}(\psi_i\phi^{(i)} - \psi_{i,a}\zeta - \psi_{i,b})\right) \tag{69}$$

The unknown functions $\psi_{i,a}$ and $\psi_{i,b}$ can be eliminated using boundary conditions and stress continuity conditions between layers. The stress state can then be expressed in terms of only the $\psi_i(\xi)$ functions for each layer. Using shear stress continuity between layers, $\psi_{i,a}$ can be expressed as:

$$\lambda_i\psi_{i,a} = \lambda_i\psi_i\phi_\zeta^{(i)}(\xi,0) - \sum_{j=1}^{i-1}\lambda_j\psi_j\left\langle\phi_{\zeta\zeta}^{(j)}\right\rangle \tag{70}$$

where averaging brackets denotes averaging over the thickness of the layer:

$$\left\langle\phi_{\zeta\zeta}^{(j)}\right\rangle = \int_0^1 d\zeta\phi_{\zeta\zeta}^{(j)} \tag{71}$$

Such averaged quantities are functions only of ξ. Similarly, using transverse stress continuity between layers and the previous $\psi_{i,a}$ result, $\psi_{i,b}$ can be expressed as:

$$\lambda_i^2\psi_{i,b} = \lambda_i^2\psi_i\phi^{(i)}(\xi,0) - \sum_{j=1}^{i-1}\lambda_j\psi_j\left(\lambda_j\left\langle\int_0^\zeta d\zeta'\phi_{\zeta\zeta}^{(j)}\right\rangle + \lambda_{ji}\left\langle\phi_{\zeta\zeta}^{(j)}\right\rangle\right) \tag{72}$$

where λ_{ji} (see Eq. (8)) is the dimensionless distance from the right edge of layer j to the left edge of layer i (note that $\lambda_{j,j+1} = 0$). The averaged term in Eq. (72) came from

$$\left\langle\phi_\zeta^{(i)}\right\rangle - \phi_\zeta^{(i)}(\xi,0) = \int_0^1 d\zeta'\phi_\zeta^{(i)}(\xi,\zeta') - \int_0^1 d\zeta'\phi_\zeta^{(i)}(\xi,0) = \int_0^1 d\zeta'\int_0^{\zeta'} d\zeta''\phi_{\zeta\zeta}^{(i)} = \left\langle\int_0^\zeta d\zeta'\phi_{\zeta\zeta}^{(i)}\right\rangle \tag{73}$$

Substituting $\psi_{i,a}$ and $\psi_{i,b}$ into the general stress function in Eq. (67), the stress function for layer i can be written as

$$\Phi^{(i)} = t_i^2\left[\phi^{(i)} - \Psi_i\omega_i - \frac{1}{\lambda_i^2}\sum_{j=1}^{i-1}\lambda_j\Psi_j\left(\lambda_i\zeta + \lambda_{ji} + \lambda_j\left\langle\omega_{j,\zeta}\right\rangle\right)\right] \tag{74}$$

where $\omega_i(\xi,\zeta)$ is a function of ξ and ζ and $\Psi_i(\xi)$ is a function only of ξ. These new functions are defined in terms ψ_i and the initial stress function $\phi^{(i)}$ (see Eq. (8)). A second subscript "ζ" on $\omega_i(\xi,\zeta)$ denotes partial differentiation with respect to ζ.

Now Eq. (74) is general for any arbitrary initial stress state. When, as always assumed in this paper, the initial stresses are independent of ξ (which implies that $\omega_i(\xi,\zeta)$ is independent of ξ), the perturbation stresses become

$$\sigma_{xx,p}^{(i)} = -\Psi_i\omega_{i,\zeta\zeta} \tag{75}$$

$$\sigma_{xz,p}^{(i)} = \lambda_i\Psi_i'\omega_{i,\zeta} + \sum_{j=1}^{i-1}\lambda_j\Psi_j' \tag{76}$$

$$\sigma_{zz,p}^{(i)} = -\lambda_i^2\Psi_i''\omega_i - \sum_{j=1}^{i-1}\lambda_j\Psi_j''\left(\lambda_i\zeta + \lambda_{ji} + \lambda_j\left\langle\omega_{j,\zeta}\right\rangle\right) \tag{77}$$

where

$$\omega_{i,\zeta} = \frac{\partial\omega_i}{\partial\zeta} = \frac{\int_0^\zeta d\zeta'\phi_{\zeta\zeta}^{(i)}}{\left\langle\phi_{\zeta\zeta}^{(i)}\right\rangle} \quad \text{and} \quad \omega_{i,\zeta\zeta} = \frac{\partial^2\omega_i}{\partial\zeta^2} = \frac{\phi_{\zeta\zeta}^{(i)}}{\left\langle\phi_{\zeta\zeta}^{(i)}\right\rangle} \tag{78}$$

The Ψ_i functions for the n layers are not entirely independent; they are constrained by the need to maintain force and moment balance on the entire structure. The initial stresses must themselves satisfy force and moment balance with the applied forces and moments. The perturbation stresses must provide no additional forces or moments; thus

the perturbation stress must have zero net force and zero net moment. The x-direction force balance and moment balance conditions for the perturbations stresses are thus:

$$x \text{ axis force balance}: \qquad \sum_{i=1}^{n} \int_{z_0^{(i)}}^{z_f^{(i)}} dz\, \sigma_{xx,p}^{(i)} = 0 \tag{79}$$

$$x \text{ axis moment balance}: \qquad \sum_{i=1}^{n} \int_{z_0^{(i)}}^{z_f^{(i)}} dz\, \sigma_{xx,p}^{(i)}(z - z_{mid}) = 0 \tag{80}$$

where $z_0^{(i)}$ and $z_f^{(i)}$ are the initial and final z coordinates of layer i and z_{mid} is the midpoint of the structure. Substituting the perturbation stresses, these two conditions can be expressed as in Eqs. (9) and (10), respectively.

Without repeating the numerous algebraic manipulations, Eqs. (75)–(77) can be verified to be a valid admissible stress state by verifying that the stresses satisfy stress equilibrium, that the shear and transverse stresses are continuous between layers, and that the shear and transverse perturbation stresses are zero on the boundaries (at the start of layer 1 and at the end of layer n). This verification is facilitated by noting that $\omega_i(0) = \omega_{i,\zeta}(0) = 0$, $\omega_i(1) = \langle \omega_{i,\zeta} \rangle$ and $\omega_{i,\zeta}(1) = 1$ and by using the force and moment balance conditions in Eqs. (9) and (10).

5.2. Complementary Energy in n Layers

The total complementary energy for an a n-layered specimen with x-independent initial stresses subjected only to tractions (*i.e.*, no displacement boundary conditions) is:

$$\Gamma = \sum_{i=1}^{n} \frac{W}{2} \int_{x_i}^{x_f} dx \int_{z_0^{(i)}}^{z_f^{(i)}} dz\, \vec{\sigma}^{(i)} \cdot \mathbf{K}^{(i)} \vec{\sigma}^{(i)} = \sum_{i=1}^{n} \frac{W \lambda_i t_*^2}{2} \int_{\xi_i}^{\xi_f} d\xi \int_0^1 d\zeta\, \vec{\sigma}^{(i)} \cdot \mathbf{K}^{(i)} \vec{\sigma}^{(i)} \tag{81}$$

where W is the width of the structure in the y direction, x_i, x_f, ξ_i, and ξ_f are the initial and final dimensioned and dimensionless coordinates of layer i in the x direction, and $\mathbf{K}^{(i)}$ is the compliance tensor of the material in layer i. We assume each layer is at least orthotropic and that the x and z directions are along principal material directions. We further assume plane stress conditions or zero stress in the y direction (note that a plane strain solution can be trivially derived from the plane stress analysis by replacing layer mechanical properties by appropriately reduced mechanical properties). For such orthotropic layers $\mathbf{K}^{(i)}$ for x-z plane stresses is given by

$$\mathbf{K}^{(i)} = \begin{pmatrix} K_{xx}^{(i)} & K_{xz}^{(i)} & 0 \\ K_{xz}^{(i)} & K_{zz}^{(i)} & 0 \\ 0 & 0 & K_{ss}^{(i)} \end{pmatrix} = \begin{pmatrix} \frac{1}{E_{xx}^{(i)}} & -\frac{\nu_{xz}^{(i)}}{E_{xx}^{(i)}} & 0 \\ -\frac{\nu_{xz}^{(i)}}{E_{xx}^{(i)}} & \frac{1}{E_{zz}^{(i)}} & 0 \\ 0 & 0 & \frac{1}{G_{xz}^{(i)}} \end{pmatrix} \tag{82}$$

where E, G, and ν are the tensile and shear moduli and Poison's ratio of layer i.

When the stresses in a cracked body partition into initial stresses and perturbation stresses, Hashin [16, 17] has proven that the complementary energy be written as

$$\Gamma = \Gamma_0 + \sum_{i=1}^{n} \frac{W \lambda_i t_*^2}{2} \int_{\xi_i}^{\xi_f} d\xi \int_0^1 d\zeta\, \vec{\sigma}_p^{(i)} \cdot \mathbf{K}^{(i)} \vec{\sigma}_p^{(i)} \tag{83}$$

where Γ_0 is the complementary of the undamaged sample

$$\Gamma_0 = \sum_{i=1}^{n} \frac{W \lambda_i t_*^2}{2} \int_{\xi_i}^{\xi_f} d\xi \int_0^1 d\zeta\, \vec{\sigma}_0^{(i)} \cdot \mathbf{K}^{(i)} \vec{\sigma}_0^{(i)} \tag{84}$$

and $\vec{\sigma}_0^{(i)}$ and $\vec{\sigma}_p^{(i)}$ are the initial and perturbation stresses, respectively. This general result simplifies the analysis. To minimize the complementary energy of the damaged sample we can ignore the initial stress state which only contributes to the constant term Γ_0. We only need to minimize the energy calculated from the perturbation stresses.

The general perturbation stresses for x-independent initial stresses are given in Eqs. (75)–(77). Substituting these stresses into Eq. (83) and rearranging, the total complementary energy of a n-layered specimen can be written as:

$$\Gamma_p = W t_*^2 \sum_{i=1}^{n} \lambda_i \int_{\xi_i}^{\xi_f} d\xi \sum_{j=1}^{i} \sum_{k=1}^{i} \Big(C_{1,ijk} \Psi_j \Psi_k + C_{2,ijk} \Psi_j'' \Psi_k + C_{3,ijk} \Psi_j'' \Psi_k'' + C_{4,ijk} \Psi_j' \Psi_k' \Big) \tag{85}$$

where

$$C_{1,ijk} = \begin{cases} \frac{1}{2}K_{xx}^{(i)}\left\langle \omega_{i,\zeta\zeta}^2 \right\rangle & j=k=i \\ 0 & \text{otherwise} \end{cases} \tag{86}$$

$$C_{2,ijk} = \begin{cases} \lambda_i^2 K_{xz}^{(i)}\left(\langle\omega_{i,\zeta}\rangle - \left\langle \omega_{i,\zeta}^2 \right\rangle\right) & j=k=i \\ \lambda_j K_{xz}^{(i)}\left(\lambda_i\left(1-\langle\omega_{i,\zeta}\rangle\right) + \lambda_{ji} + \lambda_j\langle\omega_{j,\zeta}\rangle\right) & j\neq i,\ k=i \\ 0 & \text{otherwise} \end{cases} \tag{87}$$

$$C_{3,ijk} = \begin{cases} \frac{1}{2}\lambda_i^4 K_{zz}^{(i)}\left\langle \omega_i^2 \right\rangle & j=k=i \\ \lambda_i^2\lambda_j K_{zz}^{(i)}\left(\lambda_i\langle\omega_i\zeta\rangle + \lambda_{ji}\langle\omega_i\rangle + \lambda_j\langle\omega_{j,\zeta}\rangle\langle\omega_i\rangle\right) & j\neq i,\ k=i \\ 0 & j=i,\ k\neq i \\ \frac{1}{2}\lambda_j\lambda_k K_{zz}^{(i)}\left[\left(\frac{1}{2}\lambda_i + \lambda_{ji} + \lambda_j\langle\omega_{j,\zeta}\rangle\right)\left(\frac{1}{2}\lambda_i + \lambda_{ki} + \lambda_k\langle\omega_{k,\zeta}\rangle\right) + \frac{1}{12}\lambda_i^2\right] & j\neq i,\ k\neq i \end{cases} \tag{88}$$

$$C_{4,ijk} = \begin{cases} \frac{1}{2}\lambda_i^2 K_{ss}^{(i)}\left\langle \omega_{i,\zeta}^2 \right\rangle & j=k=i \\ \lambda_i\lambda_j K_{ss}^{(i)}\langle\omega_{i,\zeta}\rangle & j\neq i,\ k=i \\ 0 & j=i,\ k\neq i \\ \frac{1}{2}\lambda_j\lambda_k K_{ss}^{(i)} & j\neq i,\ k\neq i \end{cases} \tag{89}$$

5.3. Solution to Euler Equation

There are two solutions to Eq. (19) depending on the relative values of p and q. When $4q/p^2 > 1$

$$\begin{aligned} \psi(\xi) \quad = \quad & \frac{2(\beta\sinh\alpha\rho\cos\beta\rho + \alpha\cosh\alpha\rho\sin\beta\rho)}{\beta\sinh 2\alpha\rho + \alpha\sin 2\beta\rho}\cosh\alpha\xi\cos\beta\xi \\ & + \frac{2(\beta\cosh\alpha\rho\sin\beta\rho - \alpha\sinh\alpha\rho\cos\beta\rho)}{\beta\sinh 2\alpha\rho + \alpha\sin 2\beta\rho}\sinh\alpha\xi\sin\beta\xi \end{aligned} \tag{90}$$

where

$$\alpha = \frac{1}{2}\sqrt{2\sqrt{q} - p} \qquad \text{and} \qquad \beta = \frac{1}{2}\sqrt{2\sqrt{q} + p} \tag{91}$$

When $4q/p^2 < 1$

$$\psi(\xi) = \frac{\tanh\alpha\rho\tanh\beta\rho}{\beta\tanh\beta\rho - \alpha\tanh\alpha\rho}\left[\frac{\beta\cosh\alpha\xi}{\sinh\alpha\rho} - \frac{\alpha\cosh\beta\xi}{\sinh\beta\rho}\right] \tag{92}$$

where

$$\alpha = \sqrt{-\frac{p}{2} + \sqrt{\frac{p^2}{4} - q}} \qquad \text{and} \qquad \beta = \sqrt{-\frac{p}{2} - \sqrt{\frac{p^2}{4} - q}} \tag{93}$$

The function $\chi(\rho)$ used in defining the energy (see Eq. (21)) also has two forms. When $4q/p^2 > 1$

$$\chi(\rho) = 2\alpha\beta(\alpha^2+\beta^2)\frac{\cosh 2\alpha\rho - \cos 2\beta\rho}{\beta\sinh 2\alpha\rho + \alpha\sin 2\beta\rho} \tag{94}$$

where α and β are given by Eq. (91). When $4q/p^2 < 1$

$$\chi(\rho) = \alpha\beta(\beta^2-\alpha^2)\frac{\tanh\alpha\rho\tanh\beta\rho}{\beta\tanh\beta\rho - \alpha\tanh\alpha\rho} \tag{95}$$

where α and β are given by Eq. (93). Notice that the specific forms for α and β are different for the two possible solutions. McCartney has solved this same equation but expressed the results in a different form [21]. The solution here can be shown to be identical to McCartney's [21] solution.

References

1. Nairn, J. A. and S. R. Kim, A Fracture Mechanics Analysis of Multiple Cracking in Coatings. *Eng. Fract. Mech.*, 1992, **42**, 195–208.
2. Kim, S. R., *Fracture Mechanics Approach to Multiple Cracking in Paint Films*, M.S. Thesis, University of Utah, 1989.
3. Kim, S. R., *Understanding Cracking Failures of Coatings: A Fracture Mechanics Approach*, Ph.D. Thesis, University of Utah, 1993.

4. So, P. and L. J. Broutman, The Effect of Surface Embrittlement on the Mechanical Behavior or Rubber-Modified Polymers. *Polym. Engng. Sci.*, 1982, **22**, 888–894.
5. Rolland, L. and L. J. Broutman, Surface Embrittlement of Ductile Polymers: A Fracture Mechanics Analysis. *Polym. Engng. Sci.*, 1985, **25**, 207–211.
6. So, P. K. and L. J. Broutman, The Fracture Behavior or Surface Embrittled Polymers. *Polymer Engng and Science*, 1986, **26**, 1173–1179.
7. Crouch, B. A., The Mechanics of Surface Embrittlement of Polymers. *Materials and Mechanics Issues, ASME*, 1993, 339–350.
8. Verpy, C, J. L. Gacougnolle, A. Dragon, A. Vanlerberghe, A. Chesneau, and F. Cozette, The Surface Embrittlement of a Ductile Blend due to a Brittle Paint Layer. *Progress in Organic Coatings*, 1994, **24**, 115–129.
9. Hsieh, A. J., P. Huang, S. K. Venkataraman, and D. L. Kohlstedt, Mechanical Characterization of Diamond-Like Carbon (DLC) Coated Polycabonates. *Mat. Res. Cos. Symp. Proc.*, 1993, **308**, 653–658.
10. *Tensile Properties of Organic Coatings*, ASTM D-2370, 1982.
11. *Paint Testing Manual*, Sward, G. G., editor, ASTM STP 500, 1972.
12. Durelli, A. J., E. A. Phillips, and C. H. Tsao, Properties of Stress Coat. *Analysis of Stress and Strain*, McGraw-Hill, 1958, 375–431.
13. Kim, S. R. and J. A. Nairn, Fracture Mechanics Analysis of Coating/Substrate Systems: II. Experiments in Bending. *Engr. Fract. Mech.*, 2000, **in press**.
14. McCartney, L. N. and C. Pierce, Stress Transfer Mechanics for Multiple Ply Laminates for Axial Loading and Bending. *Proc. ICCM-11*, Gold Coast, Australia, 1997.
15. McCartney, L. N. and C. Pierce, Stress Transfer Mechanics for Mulitple Ply Laminates Subject to Bending. *NPL Report CMMT(A)55*, 1997.
16. Hashin, Z., Analysis of Cracked Laminates: A Variational Approach. *Mech. of Mat.*, 1985, **4**, 121–136.
17. Hashin, Z., Analysis of Stiffness Reduction of Cracked Cross-Ply Laminates. *Eng. Fract. Mech.*, 1986, **25**, 771–778.
18. Nairn, J. A., The Strain Energy Release Rate of Composite Microcracking: A Variational Approach. *J. Comp. Mat.*, 1989, **23**, 1106–1129. (see errata: *J. Comp. Mat.*, 1990, **24**, 233).
19. Nairn, J. A., S. Hu, and J. S. Bark, A Critical Evaluation of Theories for Predicting Microcracking in Composite Laminates. *J. Mat. Sci.*, 1993, **28**, 5099–5111.
20. Nairn, J. A. and S. Hu, Micromechanics of Damage: A Case Study of Matrix Microcracking. *Damage Mechanics of Composite Materials*, ed., Ramesh Talreja, Elsevier, Amsterdam, 1994, 187–243.
21. McCartney, L. N., Theory of Stress Transfer in a 0-90-0 Cross-Ply Laminate Containing a Parallel Array of Transverse Cracks. *J. Mech. Phys. Solids*, 1992, **40**, 27–68.
22. Nairn, J. A., A Variational Mechanics Analysis of the Stresses Around Breaks in Embedded Fibers. *Mech. of Materials*, 1992, **13**, 131–154.
23. Nairn, J. A., Fracture Mechanics of Composites With Residual Thermal Stresses. *J. Applied Mech.*, 1997, **64**, 804–810.
24. Hashin, Z., Finite Thermoelastic Fracture Criterion with Application to Laminate Cracking Analysis. *J. Mech. Phys. Solids*, 1996, **44**, 1129–1145.
25. Crandall, S. H., Dahl, N. C., and Lardner, T. J., *An Introduction to the Mechanics of Solids*, McGraw-Hill, New York, 1978.
26. Mathematica Version 2.2, Wolfram Research, Champaign, Illinois, 1994.
27. Varna, J. and L. A. Berglund, A Model for Prediction of the Transverse Cracking Strain in Cross-Ply Laminates. *J. Reinf Plast. and Comp.*, 1992, **11**, 708–728.
28. Varna, J. and L. Berglund, Multiple Transverse Cracking and Stiffness Reduction in Cross-Ply Laminates. *J. Comp. Tech. & Res.*, 1991, **13**, 97–106.
29. McCartney, L. N., Stress Transfer Mechanics for Ply Cracks in General Symmetric Laminates. *NPL Report CMMT(A)50*, 1996.